Scientific report; WR 2010-01

Dynamics of the marine atmospheric boundary layer at high wind conditions

Vladimir Kudryavtsev and Vladimir Makin

February 2010

Scientific report = Wetenschappelijk rapport; WR 2010-01

De Bilt, 2010

P.O. Box 201
3730 AE De Bilt
Wilhelminalaan 10
Telephone +31 30 220 69 11
Telefax +31 30 221 04 07

● ● ● ●

Scientific report; WR 2010-01

Dynamics of the marine atmospheric boundary layer at high wind conditions

Vladimir Kudryavtsev and Vladimir Makin

February 2010

Abstract

The impact of ocean spray on the dynamics of the marine atmospheric boundary layer (MABL) in conditions of very high (hurricane) wind speeds is investigated. To that end a model of the MABL in presence of sea spume spray is constructed. The model is based on the classical theory of the motion of suspended particles in a turbulent flow, where the mass concentration of droplets is not mandatory small. A description of the spume droplets generation in the model assumes that they being torn off from breaking waves are injected in the form of a jet of spray into the airflow at the altitude of breaking crests. The distribution of droplets inside the jet is proportional to the radius to the power 2; the total production of droplets is proportional to the length of wave breaking fronts. Droplets affect the MABL dynamics in two ways: via redistribution of the momentum between droplets and air forming the so-called spray stress, and via the impact of droplets on the turbulent mixing through stratification. The latter is parameterized through the extension of the Monin-Obukhov similarity theory. At high wind speeds the tearing off shortest breaking wave crests results in the appearance of the near surface sheet of spray with the mixture density exceeding the air density in few times. The spray stress mechanism *per se* leads to the increase of the momentum flux in the MABL. The dominant impact of droplets on the MABL dynamics appears through stratification. That leads to the suppression of the turbulent mixing and the momentum flux in the MABL and, as a consequence, to the acceleration of the wind velocity and the suppression of the sea surface drag. Model results are consistent with observations.

Contents

1. Introduction

As a result of increasing frequency and intensity of tropical cyclones (see, e.g., Black et al., 2007), an accurate forecasting of cyclone evolution and ocean response is becoming of principle importance in reduction threats to human lives and property in coastal regions. The energy exchange at the air-sea interface is one of major physical processes governing hurricane intensity change. The air-sea exchanges of heat, moisture and momentum determines how hurricanes gain their strength and intensity from the ocean (Black et al., 2007). On the other hand these exchanges, of momentum in the first place, determine the response of the ocean resulting in storm surges, waves and currents. While efforts to forecast hurricane tracks have improved greatly, the ability to forecast hurricanes intensity has shown little skill (Black et al., 2007; and references there). Understanding and a proper description of the air-sea exchange processes is thus crucial in increasing quality of the tropical cyclones modeling.

The present study is aimed at better understanding of the exchange of momentum in hurricanes.

There is indirect evidence that at hurricane wind speeds the drag coefficient does not increase with the increasing wind. Modelling studies of the tropical cyclone storms (e.g., Emanuel, 1995; Frank, 1984; Kaplan and Frank, 1993) showed, that cyclones cannot attain their observed intensity with traditional parameterizations of the drag coefficient, and it is necessary ad hoc to reduce the drag. Emanuel (1995) showed, that the intensity of hurricanes depends on the magnitude of the surface exchange coefficients; in particular, the maximum wind speed in hurricanes depends on the ratio of enthalpy to the momentum exchange coefficient. That should be in the range 1.2-1.5 to explain the observed winds. The value exceeds twice a value if a traditional parameterization of the drag coefficient (linear increase with the wind speed) is used.

The saturation of the surface stress with an increasing wind speed is implicitly supported by the scatterometer measurements. Data by Donnely et al. (1999) on the C-band ocean backscatter at high wind conditions clearly showed a saturation of the backscatter power at the wind speed exceeding 25 m s^{-1}. The relation of the surface geometrical roughness (height of short waves that scatter the radio waves) to the wind surface stress is not obvious. However, if such relation does exist, the saturation of the backscatter at high wind speed presumes the decrease of the surface drag coefficient.

The first experimental evidence of the saturation of the surface drag at hurricane wind speeds was reported by Powell et al. (2003). They obtained the wind velocity profiles by releasing Global Positioning System drop wind sondes in tropical cyclones and found, that the drag coefficient levels off and starts to decrease with a further increase in the wind speed above the hurricane force of about 34 m s^{-1}. This is contrary to the traditional parameterizations that predict increase of the drag coefficient with an increasing wind speed, and supports the ad hoc capping of the drag coefficient used in the hurricane modeling.

Jarosz et al. (2007) used the so-called "bottom-up" determination of the air-sea momentum exchange under extreme wind conditions. This method is based on current measurements in the water column below a passing tropical cyclone. The drag coefficient is then obtained from the along-shelf momentum balance. The authors confirmed the finding by Powell et al. (2003): the drag coefficient peaks at a wind speed near 32 m s^{-1} and then steadily decreases as the wind speed continues to rise.

Powell et al. (2003) speculate that increased foam coverage resulting from intensively breaking waves could progressively form a 'slip' surface at the air-sea interface that leads to the reduction of the sea drag at the wind speed above 40 m s^{-1}. In addition sea spray is hypothesized to significantly influence the transfer of momentum. Their evidence is cited: 'As the wind approaches 50 m s^{-1}, the sea becomes completely covered by a layer of foam and it is difficult to discern individual wave-breaking elements in the reduced visibility from spray and rain'.

State of the Sea Card describes this regime (wind force 12, wind speed greater than 31 m s^{-1}) as: 'The air is filled with foam and spray. Sea completely white with driving spray; visibility very seriously affected.'

Postulating that ocean spray is responsible for the peculiar behavior of the drag coefficient at hurricane wind speeds we arrive at a classical problem of the two-phase fluid dynamics.

Lighthill (1999) postulated 'the need to fill gaps in knowledge about ocean spray at extreme wind speeds'. He himself was interested in the impact of spray on the thermodynamics of tropical cyclones. His study was aimed at estimating the probability distribution for the height of a particular

spray droplet after it leaves the ocean surface. He used an approach, which he called 'somewhat intermediate between the two' (statistical theory of turbulence and the Monte Carlo simulations of droplet trajectories).

In the present study we are interested in the impact of spray on the dynamics of the atmosphere, in particular, on the resistance of the sea surface. That is why we keep staying with the approach based on the statistical theory of turbulence and will not discuss other approaches.

The theory of the motion of suspended particles (spray droplets in our case) in a turbulent flow of incompressible fluid (air in our case) was developed by Barenblatt (1953, 1955) and Kolmogorov (1954) (see also monographs by, for example, Azbel (1981); Barenblatt (1996); Monin and Yaglom (1971); and the literature cited there). The fundamental postulate of the theory is the assumption that the size of the suspended particles is small in comparison with the length scales of turbulence. That permits to assume that they form a continuous distribution of mixture in the basic fluid (Monin and Yaglom, 1971). The density of the mixture is written in the form

$$\rho = \rho_a(1 - s) + \rho_w s = \rho_a + (\rho_w - \rho_a)s, \qquad (1.1)$$

where ρ_a and ρ_w are the air and the water density, s is the volume concentration of droplets. The Boussinesq approximation is used; that is the density variation (mass concentration)

$$\frac{(\rho_w - \rho_a)s}{\rho_a} = \sigma s \ll 1 \qquad (1.2)$$

is assumed to be small and is accounted for only in terms related to the action of gravity, i.e. the buoyancy force term in the equation for the turbulent kinetic energy (TKE). Here, σ is the relative excess of the particle density over the fluid density and σs is the mass concentration. For the same reason the impact of particles on the momentum balance equation is omitted.

The approach was successfully applied to several two-phase geophysical flows, e.g., dust storms (Barenblatt and Golitsyn, 1974), silts on beaches, ocean floor and river beds (Bagnold, 1962; Bridge and Dominic, 1984), drifting snow (Bintanja, 2000) and others (see original citing in mentioned references). The essence of the theory is that particles being embedded into the fluid flow form a stable stratified layer that damps the turbulent mixing and results in acceleration of the flow.

It is rather surprising that the application of the approach to the problem of sea spray in hurricanes was overlooked for quite a long time, may be because of the lack of observations.

The finding of Powell et al. (2003) boosted up several theoretical studies aiming at the explanation of the observed reduction of the sea drag. Makin (2005) (hereinafter M05) suggested that at high wind speeds above 30 m s^{-1} a thin (with thickness less than the significant wave height) atmospheric boundary layer adjacent to the surface turns to a regime of limited saturation by suspended light sea droplets (dimensionless fall velocity $\omega = a/\kappa u_* < 1$, where a is the terminal fall velocity, κ is von Karman constant and u_* is the friction velocity). At this regime the Richardson number in this layer reaches the critical value. That results in a reduction of the surface drag and acceleration of the airflow. Using the solution by Barenblatt (e.g., Barenblatt, 1996) for the flow in a regime of limited saturation and some empirical knowledge he managed to explain the reduction of the drag coefficient, as observed by Powell et al. (2003). However, the assumption that the flow turns into that regime near the surface is questionable.

Barenblatt et al. (2005) applied the general theory of suspended particles in the turbulent fluid developed by Barenblatt and Kolmogorov. They assumed that large droplets ($\omega \gg 1$) play the dominant role in the dynamics of the air flow and showed that the reduction of the turbulence intensity leads to a sharp flow acceleration. They suggested a "sandwich" model, where droplets form a thin layer with a constant concentration just below the height of breaking waves. Because the concentration of droplets vary fast with height, there exists a sharp upper boundary of the ocean spray, and the acceleration of the airflow is confined to that layer. However, the choice of the parameters they used in their example is questionable.

Kudryavtsev (2006) (hereinafter K06) followed in general lines the approach by Barenblatt and Golitsyn (1974) and developed a more elaborated model. He suggested that the effect of sea droplets on the turbulent marine atmospheric boundary layer (MABL) is similar to the effect of temperature stratification. Both affect turbulence by the similar manner - through the buoyancy force. K06 suggested to adopt the well established universal functions of the Monin-Obukhov similarity theory for the stably stratified boundary layer to describe the dynamics of the MABL in presence of spray. This approach was also used by Bye and Jenkins (2006) in their study of the surface drag at high winds. K06 found, that sea droplets of the observed concentrations cannot affect the MABL dynamics, unless one assumes, that they are injected into the airflow well above the sea surface at altitude of breaking wave crests. In order to take this into account K06 introduced the volume source of droplets in the conservation equation for spray. This term is proportional to the length of wave breaking fronts and models the generation of spume droplets, which being torn off from wave crests are then injected into the airflow at some altitude. As shown, spume droplets may significantly affect the turbulent mixing at strong wind speeds leading to acceleration of the near surface wind speed and reduction of the surface drag, similar

to that as observed by Powell et al. (2003). However, K06 noticed that results of his model depend significantly on the droplets radius, which was imposed (though in accordance with observations) and assumed independent from the wind speed . Drawbacks of such assumption was recently argued by Kudryavtsev and Makin (2009) (hereinafter KM09). The other problem mentioned in K06 is that when the effect of droplets on the surface drag becomes significant, the contribution of droplets to the mixture density becomes large and comparable with the air density. Therefore, the question how does the findings by K06 correspond to the reality remains open.

On the contrary to the referred above papers Andreas (2004) ignored the effect of sea spray on the atmospheric stratification and focused on their impact on the momentum balance in the atmospheric boundary layer. In the droplet evaporation layer he split the total stress into turbulent and spray supported parts. He postulated a heuristic relation for the surface spray flux; assuming its exponential decay with height he showed, that spray slows the 10-m wind by over 3 m s^{-1}. This is an opposite behavior to what was found in cited papers above. As found, at the wind speed of 30 m s^{-1} and less the effect of sea droplets on the surface momentum flux is negligible. However, due to a strong wind speed dependence of the sea droplets production their impact rapidly increases, and at the wind speed of 60 m s^{-1} sea droplets dominate the surface momentum balance and reduce the drag coefficient. Andreas points out that this result does not corroborate or vice versa the results by Powell et al. (2003) as they analyze different drag coefficients. Andreas's drag coefficient models the surface stress that supports the frictional drag of the air, while Powell et al. (2003) relate the total surface stress to the wind speed and thus analyze the classical drag coefficient. It seems questionable that the correct description of the atmospheric boundary layer with droplets could be done neglecting the effect of droplets stratification.

We also mention a pioneering study of the aerodynamic roughness of the water surface at extreme winds in the laboratory conditions as reported by Donelan et al. (2004). They also observed a saturation of the surface drag at the wind speed exceeding 33 m s^{-1} but for a different reason than in the open ocean. In the laboratory conditions spray does not play a significant role in the dynamics of the air flow. The separation of the airflow from continually breaking crests is suggested as a mechanism leading to the reduction of the drag coefficient. This mechanism is explained by theoretical studies by Kudryavtsev and Makin (2007) (hereinafter KM07) and Kukulka et al. (2007).

The goal of the present study is to developed a model of the impact of ocean spray on the dynamics of the MABL by generalizing our previous studies (M05; K06; KM07; KM09). The study is motivated by the following reasons. First, the assumption that the mass concentration is small ($\sigma s \ll 1$) loses its validity, when the concentration of droplets becomes significant. The momentum equation for the water-air mixture should be free of such restriction. Second, the impact of droplets on the atmospheric boundary layer dynamics is determined by their scale/radius. Therefore, a spray model is needed to describe consistently the droplets generation and their effect on turbulence. Third, most of droplets are produced by the wind tearing off the breaking wave crests generating spume droplets. In the same time the airflow separation from breaking waves affects the aerodynamic surface roughness. Therefore, a MABL model should take into account a dual effect of breaking waves that form the surface drag and produce spume droplets and that , in turn, affects the momentum and the TKE balance in the MABL.

2. Mass and momentum balance in presence of ocean spray

The present study is based on the classical theory of the motion of suspended particles in a turbulent flow of incompressible fluid developed by Barenblatt (1953, 1955) and Kolmogorov (1954). The main assumptions of the theory are the following: (i) the size of the suspended particles is small in comparison with the length scale of turbulence and (ii) the acceleration of the fluid and particles is small in comparison with the acceleration due to gravity. As a consequence of the latter assumption the horizontal velocity of droplets $u^w_{1,2}$ coincides with the horizontal velocity of the air $u^a_{1,2}$, and the vertical velocity u^w_3 differs from the vertical velocity u^a_3 of the air by a constant value of the terminal fall velocity of droplets a, i.e.

$$u^w_j = u^a_j - a\delta_{j3}, \tag{2.1}$$

where $j = 1, 2, 3$. Finally, (iii) the volume and mass concentration of droplets in the air is small, i.e. $\sigma s \ll 1$ and $s \ll 1$.

In the present paper the mass concentration of droplets σs is considered to be not mandatory small; this is the only difference with the classical formulation of the problem. Thus terms of order σs are not neglected in the momentum conservation equation (the non-Bousinesq approximation) as is done in the original formulation.

2.1 Governing equations

The governing mass and momentum conservation equations for a two-phase fluid free of the condition $\sigma s \ll 1$ are given in the Appendix. The equations are written in the Cartesian coordinate system; their direct application for the MABL above the wavy surface is not straightforward. A common convention is followed through this study: the averaged momentum and mass conservation equations over the mean water surface that characterize the interaction of the airflow with the water surface in terms of the roughness scales are used. First, the momentum and mass conservation equations for the MABL domain above the wave crests, where the use of governing equations in the Cartesian coordinate system is obvious, are considered. Then the domain adjacent to the wavy surface, where the direct use of these equation in the Cartesian system is not trivial and some additional assumptions are required, is described. Finally, the semi-empirical momentum and mass conservation equations that are valid in the full domain above and below wave breaking crests are proposed (see Appendix for details).

If wind waves are represented as a superposition of the narrow band waves with the wavenumber in the range from $\mathbf{k}$ to $\mathbf{k} + d\mathbf{k}$, the governing conservation equations read

$$\frac{\partial}{\partial z}(\overline{s'u'_3} - a\bar{s}) = dV_s, \tag{2.2}$$

$$dV_s = F_s\delta(z - h_b) = F_{0s}d_bL_b\delta(z - h_b) \tag{2.3}$$

for mass and

$$\frac{\partial}{\partial z}(\bar{\rho}\overline{u'_1u'_3}) = -d\Pi_s \tag{2.4}$$

$$d\Pi_s = \Delta p_s h_b L_b \delta(z - h_b) \tag{2.5}$$

for momentum. Hereinafter, the vertical coordinate x_3 used in the Appendix is replaced by z. In equations (2.2) - (2.5) $\overline{s'u'_3}$ and $\overline{u'_1u'_3}$ are the turbulent kinematic flux of droplets and momentum; $\bar{\rho} = \rho_a + (\rho_w - \rho_a)\bar{s}$ is the mean density of the mixture (hereinafter, the bar over the mean density and the mean droplets concentration is omitted); dV_s is the rate of spume droplets production per unit volume; $d\Pi_s$ is the force per unit volume caused by the divergence of the momentum flux; $\delta(x)$ is the Dirac delta function; h_b is the height of the breaking wave crests related to the wavenumber as $h_b/2 = \varepsilon/k$, ε being the steepness of breaking waves, taken here as $\varepsilon = 0.5$ so that $h_b = 1/k$; F_s is the flux of spume droplets from all breaking crests expressed through the length of breaking crests per unit area L_b as $F_s = F_{0s}d_bL_b$ (KM09); $d_b = \epsilon k^{-1}$ (ϵ is a small constant) is the thickness of the outlet of a jet of droplets injected into the airflow from a breaking crest at altitude $z = h_b$ (see Figure 1a in KM09); F_{0s} is the flux of droplets from unit area of a breaking crest; Δp_s is the pressure drop on the forward side of a breaking wave. Since sea droplets are injected into the airflow from breaking crests, the droplets flux $\overline{s'u'_3}$ at the surface must vanish.

2.2 Droplets production and separation stress

The injection of droplets presumes that they being torn away from a breaking crest are further accelerated to match the airflow velocity u_s in the vicinity of the wave crest. As shown by KM09, the force required to accelerate these droplets to u_s is $\rho_w F_{0s}u_s$ and equals the local turbulent wind stress over the breaking crest τ. Thus $\rho_w F_{0s}u_s = \tau$ and the spume droplets flux reads

$$F_{0s} = (\tau/\rho_w)/u_s \propto u_s. \tag{2.6}$$

Equation (2.6) describes the overall (integrated over the droplets radius) production of droplets from an individual breaking crest. The distribution of droplets over size is

defined from the balance of the restoring force associated with the surface tension force acting on the droplet surface and the dynamic pressure force associated with the turbulent velocity differential over the droplet (Kolmogorov 1949). Applying the Kolmogorov-Obukhov theory of the local structure of turbulence for the inner boundary layer over a breaking crest, where spume droplets are produced, KM09 found, that spume droplets injected into the airflow in the form of a jet have the following distribution over size

$$F_{0s} = 3(\tau/\rho_w)u_s^{-1}r_0^{-3}\int_{r<r_0} r^2 dr, \qquad (2.7)$$

where r_0 is the maximal radius of droplets

$$r_0 \propto (\gamma\nu/k)^{1/3}u_*^{-1}, . \qquad (2.8)$$

Here, γ is the surface water tension, ν is the kinematic viscosity, and $u_* = (\tau/\rho_a)^{1/2}$ is the friction velocity in the MABL.

The pressure drop Δp_s that acts on the forward side of the breaking wave, equation (2.5), was estimated by Kudryavtsev and Makin (2001) (hereinafter KM01) by using the analogy between the airflow separation (AFS) from a breaking crest and a separated flow from the backward facing step as

$$\Delta p_s = \frac{1}{2}c_1\rho u_s^2, \qquad (2.9)$$

where c_1 is a constant of $O(1)$, and u_s is the same wind velocity scale as in (2.7).

2.3 Overall impact of breaking waves

Equations (2.2) and (2.5) are valid for the narrow band surface waves with the wavenumber from $\mathbf{k}$ to $\mathbf{k} + d\mathbf{k}$. According to Phillips (1985) the length of wave breaking crests per unit area L_b can be expressed through the spectral density of the breaking fronts length $\Lambda(\mathbf{k})$ as

$$L_b = \Lambda(\mathbf{k})d\mathbf{k}. \qquad (2.10)$$

In order to find the contribution of all breaking waves on the "separation force" Π_s and on the total production of droplets V_s, equations (2.3) and (2.5) should be integrated over $\mathbf{k}$. Using the integration variable change $x = z - 1/k$ and $dk = (z - x)^{-2}dx$ after integration with the delta-function $\delta(x)$ the following equations are obtained

$$V_s(z) = \epsilon F_{0s}z^{-2}\Lambda(k)|_{k=1/z}, , \qquad (2.11)$$

$$\Pi_s(z) = \Delta p_s z^{-2}\Lambda(k)|_{k=1/z}, \qquad (2.12)$$

where $\Lambda(k)$ is integrated over all directions. A specific distribution of the breaking fronts length $\Lambda(k)$ is an open question. Not numerous field studies of the wave breaking statistics in terms of $\Lambda(\mathbf{k})$ (more precisely in terms of $\Lambda(\mathbf{c})$, where $\mathbf{c}$ is the velocity of a breaker) showed that experimental estimates of this quantity confirm the original idea by Phillips (1985) that a local balance exists between the wind energy input and the wave breaking dissipation. $\Lambda(\mathbf{k})$ can be then expressed as (Melville and Matusov 2002; Gemmrich et al. 2008)

$$\Lambda(\mathbf{k}) \propto k^{-1}(u_*/c)^2 B(\mathbf{k}) \propto k^{-1}(u_*/c)^3, \qquad (2.13)$$

where $B(\mathbf{k})$ is the saturation wave spectrum, and c is the phase speed. The latter relation results from the assumption that $B(\mathbf{k}) \propto u_*/c$. This relation is used here. We notice, however, that the choice of $\Lambda(\mathbf{k})$ may affect the following model results.

Substituting (2.13) in (2.11) and (2.12) and replacing k by $1/z$ the volume source of spume droplets and the separation force read

$$V_s(z) \propto F_{0s}\frac{u_*^2}{gz^2}B(k)|_{k=1/z}, \qquad (2.14)$$

$$\Pi_s(z) \propto \Delta p_s\frac{u_*^2}{gz^2}B(k)|_{k=1/z} \qquad (2.15)$$

at $z > 1/k_b$, and $V_s(z) = 0$ and $\Pi_s(z) = 0$ at $z < 1/k_b$. Since $F_{0s} \propto u_s$, $\Delta p_s \propto u_s^2$ and $B \propto u_*/c$ equations (2.14) and (2.15) predict the wind speed dependence of the droplets production and the AFS resistance force proportional to the power 4 and 5 correspondingly. As follows from (2.14) and (2.15) both the volume source of spume droplets production and the AFS resistance force attenuate rapidly with height. Thus the accuracy of the specification of the spectral shape of the peak of the wind-wave spectrum is not important. Therefore, we simply suggest that

$$B(k) \propto u_{10}/c \qquad (2.16)$$

at $c < c_p$, where c_p is the phase velocity at the spectral peak, which is a function of the dimensionless fetch $x = Xg/u_{10}^2$; u_{10} is the wind speed at 10-m height. The proportionality constant in (2.16) will be absorbed in other model constants.

The range of breaking waves contributing to the AFS and the range of breaking waves providing the spume droplets generation is not the same. KM01 suggested that the range of breaking waves supporting the AFS is confined by the interval $k < k_b \simeq 20$ rad m^{-1}. The shorter breaking waves generate parasitic capillaries; that prevents the appearance of the slope discontinuity leading to the AFS. The shortest waves in the interval $k < k_b$ break without the air entrainment, i.e without generation of white caps associated with the production of spume droplets. Gemmrich et al. (2007) investigated the wave breaking dynamics by tracing visible white caps. They found that the velocity of the smallest white caps was about 1 m s^{-1} that corresponds to k of order O(10) rad m^{-1}. The range of breaking waves supporting the AFS is thus of the same order but somewhat broader than the range of waves producing spume droplets. In order to avoid unnecessary complications, we define the interval $k < k_b = 20$ rad m^{-1} as a unified range of

breaking waves that provide the main contribution to both the AFS and the spume droplets production.

The droplets flux F_{0s} in (2.14) is defined by (2.7) and depends on z via the velocity scale u_s and the maximal radius of generated droplets r_0 defined by (2.8). However, as it follows from (2.14) most of droplets are produced by breaking of short waves at low altitudes. Therefore, we may ignore the dependence of F_{0s} and r_0 on z and define them for shortest breaking waves, i.e., r_0 in (2.8) is replaced by $r_b = r_0(k_b)$ and u_s in (2.7) - by $u_b = u_s(k_b^{-1})$.

The remaining question is: what is the role of dominant waves if most of droplets are produced by breaking of the equilibrium range? Dulov et al. (2002) found, that dominant waves strongly modulate the short wave breaking that leads to its strong enhancement on the dominant wave (DW) crest and almost total suppression in the trough area. It is suggested, that the production of spume droplets torn from crests of shortest breaking waves takes place on the crest of dominant waves. Kudryavtsev and Makin (2002) (hereinafter KM02) showed, that the modulation of wave breaking also leads to a strong modulation of the aerodynamic roughness; that along with the airflow undulation leads to a significant modulation of the surface stress along the DW. The amplitude and the phase of the surface stress modulation are dependent on the inverse wave-age parameter u_{10}/c_p of the DW . For wind waves characterized by $u_{10}/c_p > 1$, the enhancement of the stress takes place on the DW crest with the amplification factor equals to $(1 + \epsilon_p M_\tau)$, where ϵ_p is the DW slope, and M_τ is the modulation transfer function (MTF) for the surface stress. As shown by KM02 (see their Figure 5), at the wind speed of 10 m s^{-1} M_τ varies from $M_\tau = 0$ at $u_{10}/c_p = 1$ to $M_\tau = 5$ at $u_{10}/c_p > 3$. Thus for the typical slope of wind generated waves $\epsilon_p \approx 0.1$ this amplification factor is about 1.5. At higher wind speeds the impact of wave breaking on the aerodynamic roughness through the AFS becomes more pronounced; that, in turn, increases the droplets production through M_τ.

Therefore, we suggest, that the surface stress that tears off crests of short breaking waves on crests of the DW is amplified by a factor $(1 + \epsilon_p M_\tau)$. Governing equations describing the spume droplets production then read

$$V_s(z) = F_{0s}\frac{u_*^2}{gz^2}B(k)|_{k=1/z}, \quad (2.17)$$

$$F_{0s} = (1 + \epsilon_p M_\tau)\int_{r<r_b} dF_{0s}, \quad (2.18)$$

$$dF_{0s} = 3c_{0s}(\rho/\rho_a)^{1/2}u_* r_b^{-3} r^2, \quad (2.19)$$

$$r_b = c_r(\gamma\nu/k_b)^{1/3}u_*^{-1}, \quad (2.20)$$

where $c_{0s} = -c_s \ln^{-1}(k_b z_0)$, c_s and c_r are tuning constants, $\epsilon_p = k_p(2m_{00})^{1/2}$ is the steepness of the DW, and m_{00} is the variance of the sea surface displacement. Notice, that to derive (2.19) the following relation for the wind velocity scale u_s in (2.7) is used: $u_s(1/k_b) \equiv u_b = -(\tau/\rho)^{1/2}\kappa^{-1}\ln(k_b z_0)$ (z_0 is the roughness parameter), wherefrom equation (2.19) follows. According to (2.18)- (2.20) the overall production of spume droplets (integrated over the droplets radius) is proportional to the wind speed to the power 4, while the rate of the generation of spume droplets of a given radius (the spectrum of the spray generation function) depends on the wind speed to the power 7, equation (2.17).

The equation for the MTF M_τ was suggested by KM02 (their equation (38) with (32)). To simplify the equation, it is assumed, that the main contribution to the modulation of the aerodynamic roughness is due to the AFS modulation supported by short waves breaking. Then M_τ, suggested by KM02, approximately reads

$$M_\tau = 2(1 - 2c_p/u_{10}) + M_{wb}\tau_s/\tau, \quad (2.21)$$

where $M_{wb} \approx 20$ is the MTF for the length of wave breaking fronts (see Figure 2 from KM02), and τ_s/τ is the partial contribution of the separation stress to the total surface stress. The first term in (2.21) describes the impact of the undulation of the airflow on the surface stress modulation; the second one - the impact of the aerodynamic roughness via the AFS. An example of the model simulation of τ_s/τ at very high wind conditions is given in KM07 (their Figure 5). At $u_{10} > 20$ m s^{-1} the partial contribution of the AFS is $\tau_s/\tau \approx 0.5$. In hurricanes the inverse wave age of DW is u_{10}/c_p 2 ÷ 5. Thus at high wind conditions the surface stress that tears off crests of short breaking waves on crests of the DW can be enhanced in two times. This effect is taken into account by equation (2.18).

2.4 Mass and momentum conservation equation

Droplets

The volume source (2.17), integrated over all breaking waves, has to be substituted in the right-hand-side of the mass conservation equation (2.2) instead of its spectral analog dV_s in the wavenumber domain. The solution of this equation depends on the droplets size through the terminal fall velocity a. The production of droplets of different size is included in (2.17) through the flux of spume droplets from individual breaking waves F_{0s}, equations (2.18)-(2.19). We shall consider the mass conservation equation (2.2) for the spectral concentration, i.e., for the concentration of droplets with the radius in the range from r to $r + dr$. Hereinafter, the hat over any quantity Y denotes its spectral density (the distribution over the droplets radius). If the spectral density $\hat{Y}$ of a quantity Y is defined, its total value is $Y = \int \hat{Y} dr$. With this notation equation (2.2) with (2.17) reads

$$\frac{\partial}{\partial z}[\hat{q}_s - a(r)\hat{s}] = \hat{V}_s, \quad (2.22)$$

where $\hat{s}$ is the droplet volume concentration spectrum - the volume of droplets of radius r per unit volume of air (units m^3 m^{-3} μm^{-1}), and $\hat{q}_s$ is the turbulent flux of droplets of radius r.

Assuming that far enough from the sea surface both $\hat{s}$ and $\hat{q}_s$ vanish, equation (2.22) can be rewritten as

$$\hat{q}_s - a\hat{s} = -\hat{F}_s, \tag{2.23}$$

where $\hat{F}_s$ is the spectrum of the total volume flux F_s of droplets torn away from breaking waves, which is defined as

$$F_s = \int_z^\infty V_s dz, \tag{2.24}$$

where dimension of F_s is $m^3\ m^{-2}\ s^{-1}$, and V_s is given by (2.17). The spectral distribution of $F_s(z)$ over the droplets size $\hat{F}_s$ is imposed by the spectrum of F_{0s}, which is defined by (2.19).

Momentum

Similar to the flux of spume droplets F_s, the AFS momentum flux or the AFS stress τ_s is introduced as

$$\tau_s(z) = -\int_z^\infty \Pi(z) dz \tag{2.25}$$

with $\Pi(z)$ defined by (2.15). Notice, that τ_s is defined as negative since it is directed downward. The separation stress is strongly wind speed dependent, is characterized by the wind speed exponent being about 5, and rapidly attenuates with height. With (2.25) the momentum conservation equation (2.4) integrated over all breaking waves reads

$$\frac{\partial}{\partial z}(\rho\overline{u_1' u_3'} + \tau_s) = 0. \tag{2.26}$$

The equation shows that above the mean water surface the sum of the turbulent momentum flux and the momentum flux supported by the AFS from breaking wave crests is constant over height. Equation (2.26) with $\rho = \rho_a$ has the same form as proposed by Kukulka et al. (2007), though the relation for τ_s used by them is different from (2.25).

Well above the sea surface at $z \gg k_b^{-1}$ the impact of sea droplets on the air density is negligible, $\rho \simeq \rho_a$, and the separation stress vanishes. Thus the turbulent momentum flux is constant over height in that layer and equals to $-\rho_a u_*^2$, where u_* is the friction velocity outside the layer influenced by droplets. Then equation (2.26) takes the following form:

$$\rho_a\overline{u_1' u_3'} + \Delta\rho s(z)\overline{u_1' u_3'} + \tau_s(z) = -\rho_a u_*^2. \tag{2.27}$$

This equation differs from the momentum conservation equation for the pure fluid by the second term on the left-hand-side, which describes the impact of droplets on the airflow. According to (2.27) the relative impact of droplets is proportional to σs. Since $\sigma \propto \rho_w/\rho_a \propto 10^3$, the impact can be significant for the droplets concentration $s \propto 10^{-3}$. At height where the separation stress is negligible, equation (2.27) can be rewritten in terms of the local friction velocity $v_*^2 = -\overline{u_1' u_3'}$

$$v_*^2 = (\rho_a/\rho)u_*^2 = u_*^2/(1 + \sigma s) \tag{2.28}$$

stating, that the large concentration of droplets results in the reduction of the local friction velocity. Notice, that the term describing the effect of droplets on the momentum balance (the second term on the left-hand-side of (2.27)), the so-called "spray stress", differs from that introduced by Andreas (2004). Though both expressions for the spray stress lead to the reduction of the local friction velocity, their physical meaning is different. According to Andreas (2004), the spray stress is a force required to accelerate sea droplets that appeared in the airflow to the velocity of the airflow. In our model this force acts at the surface and leads to tearing off the breaking crest, generation of droplets and then their acceleration to the velocity of the airflow.

Equation (2.27) that describes the impact of droplets on the momentum balance is considered as a general one.

The separation stress (2.25) and the droplets flux (2.24) have similar vertical distribution, rapidly attenuating with height as $z^{-3/2}$ at $z > 1/k_b$. The effect of droplets on the MABL dynamics results from the action of the buoyancy force on the turbulent mixing described in terms of the Monin-Obukhov stratification length, equation (3.5) below. For heavy droplets the solution of equation (2.23) is $as \simeq F_s$, and the stratification parameter z/L_s that describes the effect of droplets on the MABL dynamics attenuates as $z^{-1/2}$, i.e., much slower than τ_s. Thus the layer affected by the AFS is thinner than the layer affected by droplets. In the context of the present study, focused on the study of the effect of droplets on the MABL dynamics, the AFS is considered as a sub-grid process and parameterized through the aerodynamic roughness scale z_0, as suggested by KM01; and by KM07 for the high wind speed conditions. As shown in these studies, the effect of the AFS can be incorporated in the Charnock roughness scale constant $c_h = z_0 g/u_*^2$. At moderate to strong wind speed up to $u_{10} = 20\ m\ s^{-1}$ c_h grows due to the strong wind speed dependence of the AFS, but at higher wind speed c_h is saturated due to the sheltering effect. Thus the effect of the AFS is included through the aerodynamic roughness prescribed by the Charnock relation

$$z_0 = c_h u_*^2/g \tag{2.29}$$

with $c_h = 0.014$.

It is important to note the following: the aerodynamic roughness z_0 is directly related to the geometrical properties of the sea surface that provide the form drag. According to the model by KM01, the aerodynamic roughness z_0 is related to the geometric properties of the wind waves expressed in terms of the saturation spectrum B as (see their equation (28)

integrated over all directions)

$$\int \ln(\pi/kz_0) B d\ln k + C_s \int \ln(\pi/kz_0)(u_s/c)^2 B d\ln k = const, \quad (2.30)$$

where C_s is the separation constant, and u_s, as before, is the wind velocity at the altitude of a breaking crest. The solution of this equation defines z_0 as a functional of B, which, as shown by Kudryavtsev and Makin (2007), can be parameterized by (2.29). In the present study the saturation spectrum is prescribed by (2.16), which at a specified reference wind speed is not dependent on the MABL stratification. Therefore, aiming at the study of the impact of droplets on the MABL dynamics, we have to assume that the aerodynamic roughness is independent of stratification. Though equation (2.30) predicts a weak dependence of z_0 on stratification via u_s, we nevertheless ignore this fact and suggest that the aerodynamic roughness is defined by (2.29), where u_* is determined by the reference conditions, i.e., without spray effect. An accurate account for the aerodynamic properties of the sea surface presumes a solution of the coupled model based on the momentum conservation equation (2.26) with the AFS flux defined by (2.25), but that is out of scope of the present study.

3. The model

3.1 Closure hypotheses

In order to close the mass and momentum conservation equations (2.2) - (2.5) we follow Barenblat (1953, 1954), Kolmogorov(1954) and Barenblat and Golitsyn (1974), and adopt the Kolmogorov-Prandtl closure hypotheses

$$\tau \equiv -\rho\overline{u_1' u_3'} = \rho K \frac{\partial U}{\partial z}, \quad (3.1)$$

$$-\overline{s' u_3'} = c_q K \frac{\partial s}{\partial z}, \quad (3.2)$$

$$K = l e^{1/2}, \quad (3.3)$$

where K is the turbulent viscosity coefficient, c_q is the inverse turbulent Prandtl number close to $c_q = 2$ (e.g., Taylor et al. 2002), l is the mixing length, U is the mean horizontal wind velocity, and e is the turbulent kinetic energy, which is found from the TKE balance equation. As argued by K06, the effect of sea droplets and the temperature stratification on turbulence appears additively. Therefore, results of the Monin-Obukhov similarity theory for the temperature stable stratified atmospheric boundary layer can be applied to the sea droplets problem. In this case, the turbulent viscosity is defined by (3.3), where $e^{1/2} \propto v_*$ (reminding that $v_* = |\tau/\rho|^{1/2}$ is the local friction velocity), and the mixing length is

$$l = \kappa(z + z_0)/\Phi,$$
$$\Phi(z/L_s) = 1 + bz/L_s, \quad (3.4)$$

where Φ is the mixing length function, b is an empirical constant normally taken as $b = 5$, $1/L_s = \kappa g(\Delta\rho/\rho)\overline{s' u_3'}/v_*^3$ is the inverse Monin-Obukhov length scale for the turbulent flow stratified due to presence of droplets. In the definition of L_s the term $\overline{s' u_3'}$ represents the total vertical turbulent transport of droplets. Within the frame of our model this turbulent transport is a sum of the turbulent flux of droplets (term q_s in equation (2.23)) and the flux of droplets torn off from breaking crests and injected into the airflow (term F_s in equation (2.23)). Using (2.23), the inverse Monin-Obukhov scale is defined as

$$\frac{1}{L_s} = \kappa \frac{\Delta\rho}{\rho} \frac{asg}{v_*^3}. \quad (3.5)$$

Notice, that the definition of Monin-Obukhov scale (3.5) differs from a definition by K06 (his equation (21)), where the turbulent flux of droplets due to the wind tearing off breaking crests was not taken into account.

3.2 Wind and droplets profiles and the sea drag

Using the closure scheme (3.2)-(3.4), the governing equations of the problem (equations (2.23) and (2.27)) take the following form:

$$\frac{\partial U}{\partial z} = \frac{v_*}{\kappa(z + z_0)}(1 + bz/L_s) \quad (3.6)$$

for momentum (reminding her that the AFS stress τ_s is taken into account through the aerodynamic roughness and the local friction velocity v_* is defined by (2.28)) and

$$\frac{\partial s}{\partial z} = -\frac{\kappa}{v_*}\frac{\partial U}{\partial z}\omega(s - s_*) = -\omega(1 + bz/L_s)(s - s_*)/(z + z_0), \quad (3.7)$$

for the droplets concentration, where $\omega = a/(c_q \kappa v_*)$ is the dimensionless terminal fall velocity based on the local friction velocity and inverse Prandtl number, and $s_* = F_s/a$ is the dimensionless turbulent flux of droplets due to the wind tearing off breaking wave crests. The boundary condition is specified on the sea surface $z = 0$ as $\partial s/\partial z = 0$, which is equivalent to specifying $s(0) = s_*(0)$. The magnitude of the dimensionless fall velocity ω divides sea droplets into two types: the light droplets with $\omega < 1$ that can be effectively transported upward by turbulence, and heavy droplets with $\omega > 1$ that fall down to the water surface after their generation (e.g., Barenblatt, 1996).

Asymptotic solutions

In case of light droplets $\omega \ll 1$, equations (3.6) and (3.7) have a remarkable solution in the area above wave crests, i.e., above the layer of droplets generation, where $s_* = 0$. At $z \gg z_0$ and $z/L_s \ll 1$ the solution is (Prandl 1949)

$$U(z) = (v_*/\kappa)\ln z + const, \quad (3.8)$$

$$s(z) = s_r(z_r/z)^{\omega}, \quad (3.9)$$

where s_r is the predefined concentration at a reference level z_r. At $z/L_s \gg 1$ the solution of (3.6) and (3.7) defines the solution for a saturated flow (Barenblat, 1953; Barenblat and Golitsyn, 1974)

$$U(z) = \frac{v_*}{\kappa\omega}\ln z + const, \quad (3.10)$$

$$s(z) \propto bc_q\kappa^2\sigma\omega^2\frac{v_*^2}{gz}. \quad (3.11)$$

In this regime the gradient of the airflow velocity is increased (since $\omega < 1$) with respect to the background flow, and the turbulent stress is significantly suppressed. K06 showed, that for light droplets with the concentration as prescribed by Andreas (2004), the regime of the saturated flow cannot be fulfilled in real conditions.

In case of heavy droplets $\omega \gg 1$, equations (3.6) and (3.7) have

also a remarkable solution. First, the solution of (3.7) at $\omega \gg 1$ approximately reads

$$s(z) \approx F_s/a \qquad (3.12)$$

stating that the droplets concentration results from the balance of the droplets flux and the gravitational force; the vertical transport by turbulence being not efficient. At height above $z = 1/k_b$ the droplets flux approximately equals to

$$F_s \approx c_s u_{10} \left(\frac{\nu_*^2}{gz}\right)^{3/2}. \qquad (3.13)$$

The stratification parameter z/L_s is $z/L_s \approx \kappa c_s \sigma u_{10}/(gz)^{1/2}$, and the velocity gradient (3.6) reads

$$\frac{\partial U}{\partial z} \approx \frac{v_*}{\kappa z}\left[1 + c_L u_{10}/(gz)^{1/2}\right], \qquad (3.14)$$

where $c_L = 2/3\kappa\sigma c_s b$ is a constant absorbing other model constants. The solution for heavy droplets shows that the droplets concentration decreases with height as $z^{-3/2}$. The wind velocity shear above crests of shortest breaking waves at $z > 1/k_b$ increases with the wind speed; that results in acceleration of the airflow due to the suppression of the turbulent mixing.

General solutions

Most of droplets are produced by the wind tearing off breaking crests. These spume droplets are rather large, with the mean radius of about 180 μm, and they can be treated as heavy droplets with $\omega \approx 10$ (e.g., Figure 2 from K06). We may anticipate, that at some height inside the logarithmic boundary layer the concentration of sea droplets becomes so small that the stratification parameter $bz/L \ll 1$. In this case, droplets do not locally affect the wind velocity shear (3.6), and the momentum flux equals $\rho_a u_*^2$. Using (2.28) and (A.7), equation (3.6) can be rewritten as

$$\frac{\partial U}{\partial z} = \left(\frac{\rho_a}{\rho}\right)^{1/2} \frac{u_*}{\kappa(z+z_0)}(1 + bz/L_s) = \frac{u_*}{\kappa(z+z_0)}[(\rho_a/\rho)^{1/2} + bz/L_{s0}), \qquad (3.15)$$

where L_{s0} is the Monin-Obukhov length scale that unlike (3.5) is defined for the outer friction velocity u_* as

$$\frac{1}{L_{s0}} = \frac{\kappa\sigma g s a}{u_*^3}. \qquad (3.16)$$

Correspondingly, the wind velocity profile and the resistance law, relating the friction velocity in the outer region to the wind speed, apparently follow from (3.15) and read

$$\kappa U(z)/u_* = \int_{z_0}^{z+z_0} \left[(1+\sigma s)^{-1/2} + \frac{b(z' - z_0)}{L_{s0}}\right] d\ln z' \qquad (3.17)$$

and

$$C_{dh} \equiv (u_*/U_h)^2 = \kappa^2 \left[\int_{z_0}^{h} \left[(1+\sigma s)^{-1/2} + \frac{b(z' - z_0)}{L_{s0}}\right] d\ln z'\right]^{-2}, \qquad (3.18)$$

where $z' = z + z_0$ is the integration variable, C_{dh} is the drag coefficient at level h, where the spume droplets concentration is so negligibly small that $h/L_{s0} \ll 1$. It is also convenient to rewrite equations (3.17) and (3.18) in the following form:

$$\kappa U(z)/u_* = \ln(\frac{z+z_0}{z_0}) + \int_{z_0}^{z+z_0} [R + \frac{b(z' - z_0)}{L_{s0}}] d\ln z' \qquad (3.19)$$

and

$$C_{dh} \equiv (u_*/U_h)^2 = \kappa^2 \left[\ln(\frac{h}{z_0}) + \int_{z_0}^{h} [R + \frac{b(z' - z_0)}{L_{s0}}) d\ln z\right]^{-2}, \qquad (3.20)$$

where

$$R = (1+\sigma s)^{-1/2} - 1 \qquad (3.21)$$

is the spray stress factor describing the impact of droplets on the wind profile and the drag coefficient through the redistribution of the momentum flux between air and droplets. Equations (3.19) and (3.20) clearly show, that when the effect of sea droplets on the turbulence mixing is ignored (terms with z/L_{s0} in (3.19) and (3.20) are omitted), the strictly negative spray stress factor R results in the decrease of the wind velocity, as compared to the logarithmic distribution, and increase of the drag coefficient. Contrary, when the droplets concentration is small enough so that $\sigma s \ll 1$ and the spray stress factor is vanishing, the equations describe the increase of the wind velocity and decrease of the drag coefficient.

Equations (3.19) and (3.20) define the problem if the distribution of the droplets concentration $s(z)$ with height and over size is known. For that we need to solve equation (3.7) with (2.24) obeying the surface boundary condition $\partial s/\partial z = 0$ at $z = 0$. The solution reads

$$\hat{s}(z) = \hat{s}_*(z) + \int_{z_0}^{z'} \exp\left[-\int_{\zeta}^{z'} \omega\Phi d\ln\zeta'\right] a^{-1}\hat{V}_s d\zeta, \qquad (3.22)$$

where $z' = z + z_0$.

To resume: equations (3.19), (3.20) and (3.22), with the flux of droplets torn away from breaking crests given by (2.24) with (2.17), represent the closed coupled system describing the generation of sea droplets, their distribution over size and height, and the effect of droplets on the MABL dynamics and the surface drag. In section 4.2 results of the model calculation based on a solution of this coupled system will be shown.

4. Results

4.1 Solution for the droplets spray generation function specified empirically

Equations (3.19) and (3.20) define the problem if the distribution of the droplets concentration $s(z)$ with height and over size is known. For that we can solve equation (3.7) with (2.24) of the coupled sea droplets-atmosphere model or use some empirical distribution of the droplets concentration (or the spray generation function (SGF)). For the illustrative purpose the latter possibility is first chosen. Following Andreas (2004) the volume flux of droplets F_s is specified as

$$F_s(z) = c_s u_*^4 \exp(-7z/H_s), \qquad (4.1)$$

where c_s is a constant, $H_s = 4m_{00}^{1/2}$ is the significant wave height, and u_* is the friction velocity well above H_s. Notice, that equation (4.1) was originally proposed by Andreas (2004) for the droplets concentration. In this study we interpret the proposed relation in terms of the droplets flux $F_s = as$, assuming that droplets are not mandatory linked to the surface waves but can be transported upward by turbulence. In this context $F_s(z)$ is equivalent to the model droplets flux (2.24), and values of $F_s(z)$ at the surface are equivalent to the definition of the standard SGF. Thus constant $c_s = 3 \cdot 10^{-7}$ corresponds to one proposed by Andreas (2004). The model distribution of droplets over the radius in the droplets flux F_s is proportional to $\propto r^2$ (equation (2.19)) and, as argued by KM09, corresponds to the spectral shape of the empirical SGF. Therefore, we suggest that the spectral distribution of F_s, defined by (4.1), is similar to the model one and has the shape $3r^2/r_0^2$, where r_0 is the spectral cutoff of the SGF. To simulate the empirical SGF proposed by Andreas (2004) the spectral cutoff should be chosen at $r_0 = 200$ μm. In this subsection we consider the model prediction for the SGF prescribed empirically by (4.1) with the spectral distribution $3r^2/r_0^2$.

It was found that the effect of the droplets flux defined by (4.1) and the spectral cutoff at $r_0 = 200$ μm on the MABL is negligible and thus not shown here. Andreas (2004) came to the similar conclusion. To magnify the effect, he suggested a heuristic SGF, which has the same form as (4.1) but with constant c_s amplified in 10-times. In this paper the spectral SGF is used. It could be anticipated, that the main drawback of the empirical SGF is a lack of its knowledge of the largest generated droplets. The empirical cutoff of the SGF at $r_0 = 200$ μm presumes that droplets of a larger radius were not traced at the altitude of measurements because they are heavy, not transported by turbulence upward and fall down to the surface

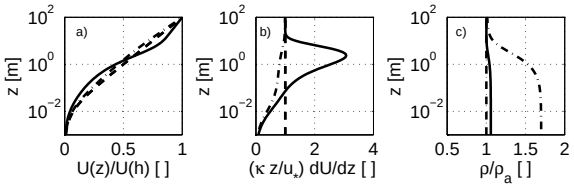

Figure 1: Empirically specified spray generation function. a) The wind profile U(z)/U(h), solid line - the spray stress and the stratification effect are accounted for; dashed-dotted line - only the spray stress is accounted for; dashed line - the reference run (no spray effect); b) The dimensionless wind shear profile defined by (3.15), line types - as in a); c) The mixture density ρ/ρ_a profile, line types- as in a). Wind speed at the reference level h = 100 m is U_h = 60 m s^{-1}.

once generated. Therefore, we suggest to increase the cutoff radius r_0 keeping however the SGF spectrum in the range $10 < r < 10^2$ μm on the original level. The modified constant c_s in (4.1) becomes to be dependent on the choice of r_0 and reads $c_s = 3 \cdot 10^{-7} r_0^3/r_{00}^3$, where r_{00} =200 μm is the original cutoff.

Following the experimental finding by Anguelova et al. (1999) we assume that the maximal radius of spume droplets is of order O(1000) μm. The model calculations with r_0 taken at 1000 μm are shown in Figure 1 and Figure 2 for the wind speed U_h = 60 m s^{-1} specified at the reference level h = 100 m. Notice that specifying c_s and r_0, we do not intend to fit the model results to any observations because these calculations are performed for the illustrative purpose only.

Dashed-dotted lines in the Figures correspond to the model calculation when the effect of droplets on the turbulence mixing is ignored (terms containing z/L_{s0} in (3.19) and (3.20) are omitted). This case is analogous to one described by the Andreas's (2004) model that accounts for the spray stress only. The presence of droplets results in the decrease of the wind shear in the whole layer as compared to the reference run (no droplets effect), where the dimensionless shear equals one, (Figure 1b). As a consequence, the wind velocity is decelerated with respect to the reference run shown in Figure 1a by a dashed line. Droplets significantly affect the mixture density,

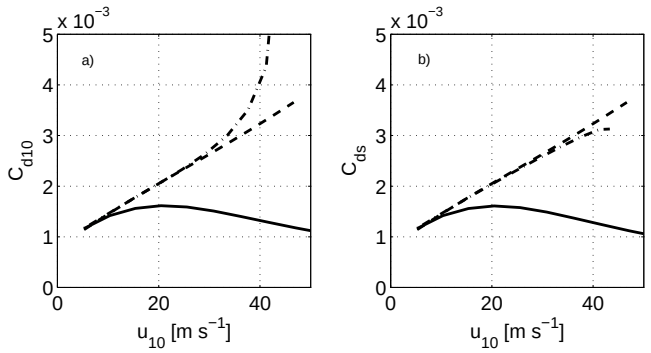

Figure 2: Empirically specified spray generation function. a) The drag coefficient at 10-m height and b) the drag coefficient at the surface versus the wind speed u_{10}; line types - as in Figure 1a.

Figure 1c; at the surface it exceeds the density of air more than in 1.5-times. The presence of droplets enhances the dynamical stress $\tau = \rho v_*^2$ in the MABL. At considered wind speed it is increased approximately in 1.5 times. Since ρv_*^2 is constant over height, the local kinematic stress v_*^2 varies with z following the profile of ρ_a/ρ, equation (2.28). At the upper level it is amplified by a factor 1.5, and at the surface it is reduced by a factor 0.75 relative to the reference value. Notice, that according to (4.1) the spray concentration depends on the friction velocity in the outer region above the spray layer. Therefore, the enhancement of the shear stress results in the enhanced production of droplets, which at $U_h = 60$ m s^{-1} leads to almost 2-times increase of the mixture density.

Solid lines in Figure 1 show model results when both the spray stress and the effect of droplets on stratification of the turbulent flow are included. The effect of droplets on stratification results in the increase of the wind velocity shear, Figure 1b, and in the significant modification of the wind velocity profile. The wind speed is accelerated at the upper levels and is decelerated near the surface due to the suppression of the turbulence mixing. The reduction of the wind stress relative to the reference and the spray-stress-only cases, in turn, results in a smaller production of droplets, as compared to the previous case. Thus the spray stress becomes negligible.

In Figure 2 the drag coefficient at 10-m height defined as $C_{d10} = (u_*/u_{10})^2$ and the drag coefficient at the surface $C_{ds} = (v_{*s}/u_{10})^2$, where v_{*s} is the friction velocity at the surface, are shown. When the effect of droplets on stratification is ignored, the presence of droplets results in the increase of C_{d10} as compared to the reference run. The surface drag coefficient C_{ds} exhibits some suppression at highest wind speeds. This suppression is artificial since the dynamical stress acting on the sea surface ρv_{*s}^2 is amplified due to the increase of the mixture density. When the effect of droplets on the MABL dynamics through stratification is accounted for, a strong reduction of both C_{d10} and C_{ds} is found. The magnitude of the reduction is comparable with one reported by Powell et al. (2002).

Thus droplets can impact the MABL dynamics in two ways: by changing the mixture density near the surface (the spray stress effect) and by changing stratification of the MABL; the latter being much more efficient. The effect of spray stress leads to deceleration of the wind speed and the enhancement of the drag coefficient that contradicts to observations by Powell et al. (2002). The impact of spray on the MABL dynamics through the effect of stratification leads to the reduction of the drag coefficient as was observed by Powell et al. (2002). In the following section this effect is investigated on the basis of the coupled droplets-atmosphere model.

4.2 Solution of the coupled sea droplets-atmosphere model

Since the description of droplets generation in the model was revised with respect to KM09, the parameters have to be redefined, and the prediction of droplets generation is compared with available data. A comprehensive review of the available empirical spume SGFs are given by Andreas (2002). It can be seen that the empirical SGFs differ from each other on several orders (more than 5) of magnitude. A plausible cause of such difference is that all of the functions are based on measurements taken in a limited range of the radius, the wind speed and at different heights above the sea level. All of them are extrapolated then to a larger radius, larger wind speed and the surface using some heuristic arguments. An example of the empirical SGF proposed by Andreas (1998) and Smith and Harrison (1998) in terms of the spectral SGF for the wind speed $u10$ of 20 m s^{-1} and 30 m s^{-1} is shown in Figure 3.

These data are used to determine the model constants c_s and c_r in the droplets production source V_s defined by (2.17)-(2.20) and the flux of droplets F_s defined by (2.24). The latter quantity is equivalent to the SGF measured at the surface. Notice, that all of the SGF measurements are made at a given altitude well above the surface. We argue, that droplets of the maximal radius could not be measured because they have a large terminal fall velocity, thus cannot be transported upward by turbulence and immediately fall back to the surface once generated. This fact could explain a rapid cutoff of the empirical spectral SGF shown in Figure 3. Therefore, the empirical SGFs cannot provide us with reliable estimate of the maximal radius of spume droplets. It is mentioned, however, that laboratory measurements by Anguelova et al. (1999) revealed the generation of spume droplets with the radius of few millimeters.

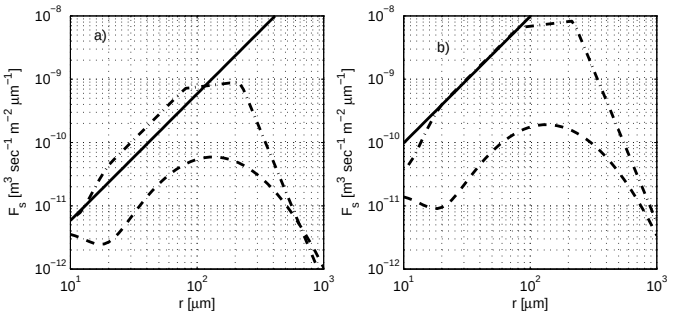

Figure 3: Spray generation function as a function of the droplets radius for the wind speed u_{10} a) 20 m s^{-1} and b) 30 m s^{-1}. Solid line, the model; dashed line, Smith and Harrison (1998); dashed-dotted line, Andreas (1998).

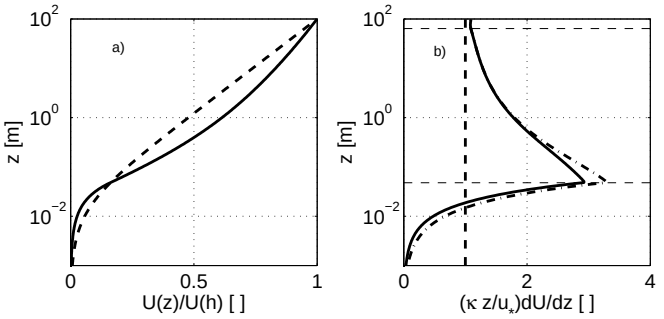

Figure 4: a) Wind profile U(z)/U(h); solid line, with spray; dashed line, without spray. b) Profile of the dimensionless wind shear defined by (3.15); solid line, with spray; dashed line, without spray; dashed-dotted line, the spray stress is switched off; thin dashed lines, altitudes from top to bottom $z = 1/k_p$ and $z = 1/k_b$. U_h = 70 m s^{-1}.

The modeled flux F_s at the surface calculated according equation (2.24) with constants $c_s = 10^{-5}$ and $c_r = 4.4$ is shown in Figure 3. The value of c_r gives the maximal radius of generated droplets about $r_b = 1800$ μm at 20 m s^{-1} and $r_b = 1100$ μm at 30 m s^{-1}. That corresponds to data reported by Anguelova et al. (1999). The value of c_s provides the level of the model SGF corresponding to the level of empirical SGFs. Notice, that at small r the model SGF has the same slope r^2 as the empirical functions. However, at large radii around $r \simeq 500$ μm the empirical SGFs have a rapid drop, while the model SGF has the cutoff at the maximal radius r_b, which is wind speed dependent. The apparent discrepancy between the model and the empirical SGF at large radii results from the fact that the model SGF is defined at the surface, while the empirical SGF is derived from measurements at some altitude. Large and heavy droplets being generated at the surface cannot be transported aloft by turbulence and are not traceable at that levels.

The wind velocity profile at U_h = 70 m s^{-1} (h = 100 m) and the vertical distribution of the dimensionless wind shear defined by (3.15) and (3.16) are shown in Figure 4. Horizontal thin dashed lines in Figure 4b indicate from top to down the altitude of breaking crests of the peak waves ($z = 1/k_p$) and crests of shortest breaking waves ($z = 1/k_b$). The maximal value of the wind shear is located approximately at the altitudes wherein droplets torn off from crests of the shortest breaking waves are injected, i.e., at $z \approx 1/k_b$. Contribution of breaking of dominant waves is small. Comparing the solid and dashed lines in Figure 4b one can conclude that the impact of the mixture density on the wind shear is not negligible, but the dominant effect of droplets on the wind profile is due to their impact on stratification and suppression of the turbulent mixing. In the layer $z > 1/k_b$ the wind shear exceeds the background one, thus the wind speed is accelerated in this layer and deviates from the reference run, Figure 4a. That in turn results in the reduction of the dynamical stress as compared to the reference run. For the wind speed considered the stress is reduced in 10-times.

Figure 5 shows the vertical distribution of the droplets concentration s, the dimensionless flux of droplets due to the wind tearing off breaking wave crests $s_* = F_s/a$ and the mixture density ρ/ρ_a. The maximum of droplets concentration and the mixture density is located at the surface. The density of the air-water mixture is considerably increased; at considered wind speed it is amplified in 4-times with respect to the density of air. According to equation (2.28) $\rho/\rho_a = u_*^2/v_*^2$ so that the distribution of the mixture density characterizes the vertical distribution of the kinematic stress v_*^2. Near the surface, where spume droplets are produced, the kinematic stress is considerably suppressed as compared to the outer layer stress u_*^2. However, the dynamical stress ρv_*^2 is constant over height and equals its value in the outer layer $\rho_a u_*^2$.

The profile of $s_*(z)$ represents the approximate solution of the mass conservation equation resulting from the balance of the spume droplets production by tearing off crests of breaking waves and their fall down due to the gravitational force (see equation(3.12)). The profile of $s(z)$ is close to $s_*(z)$ in the area where most of spume droplets are produced, i.e., in the layer $z < 1/k_p$. Above this layer the droplets concentration profile $s(z)$ deviates from $s_*(z)$ due to the increasing role of the turbulent transport of droplets.

The spectrum of the droplets concentration at different heights above the surface is shown in Figure 6. Very light droplets

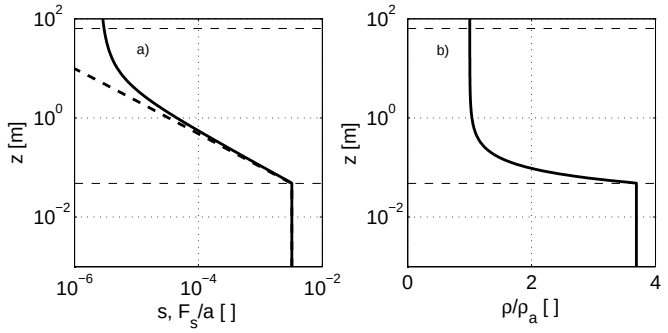

Figure 5: a) Profile of the droplets concentration s, solid line; profile of th dimensionless flux of droplets due to the wind tearing off breaking wave crests $s_* = F_s/a$, dashed line. b) Profile of the mixture density ρ/ρ_a. Thin dashed lines, as in Figure 4b. U_h = 70 m s^{-1}.

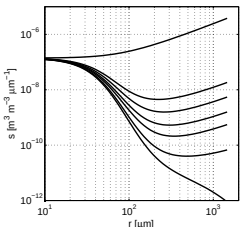

Figure 6: Spectra of the droplets concentration at different heights; lines from top to bottom correspond to heights: at the surface, 2 m, 5 m, 10 m, 20 m, 50 m, 100 m. U_h = 70 m s^{-1}.

characterized by a parameter $\omega \equiv a/\kappa v_* \ll 1$ penetrate the whole MABL as predicted by the asymptotic solution (3.8). Being generated by all breaking waves light droplets are effectively transported upward by turbulence away from the layer, where they were generated. Therefore, the vertical distribution of light droplets does not dependent on the vertical profile of $F_s(z)$, and the magnitude of light droplets concentration is defined by a value of F_s at the surface. The larger the dimensionless terminal fall velocity ω the more rapid attenuation of the droplets concentration is. Largest droplets with $\omega > 1$ are not effectively transported by turbulence. Thus their concentration essentially depends on the vertical profile of the spume droplets production. The heaviest droplets at the surface dominate the spectrum of the concentration, but their concentration rapidly decreases with height following the vertical profile of the spume droplets flux from breaking waves. Under these conditions the concentration of largest droplets decreases two orders of magnitude in the first 2 m and above 20 m these droplets are not traceable.

A standard representation of the model results in terms of the drag coefficient at 10-m height, C_{d10}, is shown in Figure 7. The reference values calculated using Charnock relation (2.29) is shown by the dashed line. The drag coefficient starts to deviate from the reference run at wind the speed above 20 m s^{-1}, and

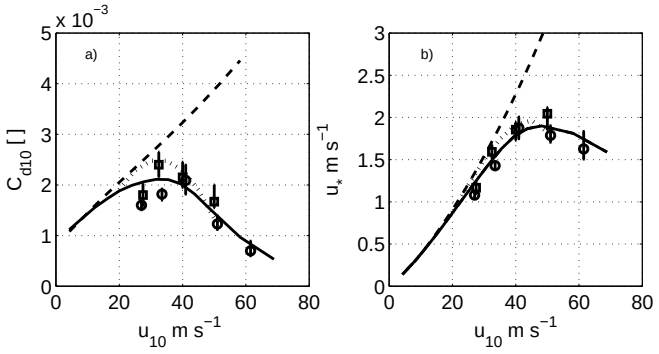

Figure 7: a) Drag coefficient and b) friction velocity versus the wind speed at 10-m height. Solid line, according to the resistance law (3.20), droplets effects are accounted for; dashed line, reference run according the Charnock relation (2.29), no droplets effects. Open circles, data by Powell (2006), compiled from his figure 7, layer 20-160 m; open squares, data by Powell et al (2003), compiled from their figure 3, layer 20-150 m; the 95% confidence limits on experimental estimates are indicated by vertical lines. Dotted line, fitted quadratic curve to the empirical data by Jarosz et al. (2007), their figure 3.

at u_{10} > 30 m s^{-1} it rapidly drops to very low values. The friction velocity peaks at about 40 m s^{-1} and with further increase in the wind speed tends to decrease also.

The model results are compared with data reported by Powell et al. (2003) and Powell (2006). We remind, that the experimental values of C_{d10}, u_* and z_0 were obtained from wind profiles measured by releasing GPS drop wind sondes. The profiles were analyzed in several layers to get reliable estimates; the estimates based on the 20-160 m surface layer are considered most reliable. These estimates are shown in Figure 7 as well. Powell et al. (2003) analyzed 331 profiles of GPS sondes dropped in 15 storms in the period 1997-1999. Their analysis determined a leveling off of the surface stress and the drag coefficient at the wind speed exceeding 34 m s^{-1} and a reduction in the roughness length. Report by Powell (2006) extends this analysis to 2664 GPS sondes profiles from the period 1997-2005. The range of the wind speed was extended up to 80 m s^{-1}. Extended data set shows a decrease of the drag coefficient to a value of about 0.5 $\cdot 10^{-3}$ above the wind speed of 40 m s^{-1} in good agreement with the present model results. The model results are also in agreement with measurements by Jarosz et al. (2007) shown by a dotted line in the same figure.

5. Conclusions

A model describing the impact of ocean spray on the dynamics of the marine atmospheric boundary layer (MABL) in conditions of very high (hurricane) wind speeds is constructed. It is based on a classical theory of the motion of suspended particles in a turbulent flow of incompressible fluid. The only difference with the classical formulation is that the mass concentration of droplets is considered to be not mandatory small. Thus terms containing the mass concentration are not neglected in the momentum conservation equation (the non-Boussinesq approximation). The derived conservation equations for mass and momentum take into account the dual effect of wave breaking on the MAL dynamics: the generation of spume droplets and the effect of the air flow separation.

The impact of spume droplets on the airflow is modeled by the source term incorporated into the mass conservation equation. The model of the spume droplets production assumes that droplets being torn off from crests of breaking wind waves are injected into the airflow at the altitude of these breaking waves. The pulverization of the water/foam into droplets takes place in a thin boundary layer adjacent to each of the breaking wave crest. Adopting Kolmogorov's (1949) ideas it is shown that the distribution of droplets over the radius in the range from 10 μm to few millimeters inside the jet is proportional to the radius to the power 2. That is consistent with measurements. The total volume production of droplets is related to the length of wave breaking fronts, where the main contribution is coming from breaking of the equilibrium range of wind waves. The overall production of spume droplets (integrated over the droplets radius) is proportional to the wind speed to the power 4, while the rate of the generation of spume droplets of a given radius (the spectrum of the spray generation function) depends on the wind speed to the power 7.

Sea droplets as a heavy particles suspended in the airflow lead to the deviation of the air-droplets mixture density from the air density. That affects the MABL dynamics in two ways: via redistribution of the momentum between droplets and air and via the impact of droplets on the turbulent mixing through stratification. The former mechanism naturally enters the governing momentum conservation equation written in the non-Boussinesq approximation. The latter mechanism enters the problem via the effect of droplets on the buoyancy force in the TKE balance and is parameterized through the extension of the Monin-Obukhov similarity theory for the stably stratified boundary layer.

Parameters of the spray generation were chosen so that to fit the empirical data as reported by Andreas (1998). It is shown that at high wind speeds the tearing off shortest breaking wave crests results in the appearance of a sheet of spray near the surface, where the density of the droplets-air mixture can exceed the air density in few times. At altitudes above crests of shortest breaking waves the density rapidly attenuates with increasing height. The behavior of the spectrum of droplets concentration with height essentially depends on the size of droplets. Light droplets with dimensionless fall velocity $\omega < 1$ are effectively transported upward by turbulence, and their vertical distribution does not depend on the vertical profile of the droplets production. Contrarily, heavy droplets with $\omega \gg 1$ could not be transported by turbulence aloft and fall back to the surface; their concentration essentially depends on the vertical profile of the production of droplets and rapidly decreases with height.

A sufficient deviation of the mixture density from the air density results in the redistribution of the momentum between droplets and air; that, in turn, leads to the deceleration of the airflow in the near surface layer, where the concentration of droplets is maximal. This mechanism alone, without accounting for the impact of droplets on stratification, leads to the increase of the dynamical surface stress that is equivalent to the enhancement of the sea surface drag. The local friction velocity v_* is however decreased, which may be mistakenly treated as the suppression of the surface drag. It is emphasized that only the dynamical stress $\tau = \rho v_*^2$ has the physical meaning.

The main impact of droplets on the MABL dynamics comes from their effect on the turbulent mixing through stratification. Contrary to the spray stress effect confined to a very thin near surface layer, the effect of spray via stratification spans higher layers and dominates the overall impact of spray on the MABL. The effect of droplets via this mechanism results in the suppression of the turbulent mixing and the momentum flux in the MABL and, as a consequence, to the acceleration of the wind velocity and suppression of the sea surface drag. It is shown that the drag coefficient levels off at the wind speed around 30 m s^{-1} and further decreases with increasing wind speed. At the wind speed of about 60 m s^{-1} the drag coefficient is considerably reduced demonstrating the effect of the "slippery surface". These features are in agreement with recent experimental data by Powell et al. (2003), Powell (2006) and Jaroz et al. (2007) acquired in hurricanes.

Acknowledgements

ONR Grant N00014-08-1-0609 and RFBR Grant N08-05-13581 are gratefully acknowledged.

Bibliography

Andreas, E. L., 1998: A new spray generation function for wind speeds up to 32 m/s. *J. Phys. Oceanogr.*, **28**, 2175–2184.

Andreas, E.L., 2002: A review of the sea spray generation function for the open ocean. *Atmosphere-Ocean Interactions, 1,* W. Perrie, Ed., WIT Press, 1-46.

Andreas, E.L., 2004: Spray stress revised. *J. Phys. Oceanogr.*, **34**, 1429-1440.

Anguelova, M., Barber, R.P. and J. Wu, 1999: Spume drops produced by the wind tearing of wave crests. *J. Phys. Oceanogr.*, **29**, 1156-1165.

Azbel, D., 1981: *Two-phase flows in chemical engineering*. Cambridge Univ. Press, Cambridge, 336 pp.

Bagnold, R. A., 1962: Autosuspension of transported sediment: Turbidity currents. *Proc. R. Soc. London*, **265**, 315-319.

Barenblatt, G.I., 1953: On the motion of suspended particles in a turbulent flow. *Prikl. Mat. Mekh.,* **17**,261-274.

Barenblatt, G. I., 1955: On the motion of suspended particles in a turbulent flow in a half-space or a plane open channel of finite depth. *Prikl. Mat. Mekh.,* **19**, 61-88.

Barenblatt, G.I., 1996: *Scaling, Self-Similarity, and Intermediate Asymptotics*. Cambridge University Press, 386 pp.

Barenblatt, G.I., and G.S. Golitsyn, 1974: Local structure of mature dust storms. textit J. Atmos. Sci.,**31**, 1917-1933.

Barenblatt, G.I., Chorin, A.J., and V.M. Prostokishin, 2005: A note concerning the Lighthill "sandwich model" of tropical cyclones. *Proc. Nat. Acad. Sc.*, **102**, 11148-11150.

Belcher, S.E., and J.C.R. Hunt, 1993: Turbulent shear flow over slowly moving waves. *J. Fluid Mech.*, **251**, 109-148.

Bintanja, R., 2000: Snowdrift suspension and atmospheric turbulence. Part I: Theoretical background and model description. *Boundary-Layer Meteorol.*, **95**, 343-368.

Black, P.G., D'Asaro, E.A., Drennan, W.M., French, J.R., Niiler, P.P., Sanford, T.B., Terrill, E.J., Walsh, E.J., and J.A. Zhang, 2007: Air-sea exchange in hurricanes. Synthesis of observations from the coupled boundarylayer air-sea transfer experiment. *Bull. Amer. Meteor. Soc.*, **88**, 357-374.

Bridge, J.S., and D.F. Dominic, 1984: Bed load velocities and sediment transport rates. *Water Resour. Res.*, **20**, 476-490.

Bye, J.A.T., and A.D. Jenkins, 2006: Drag coefficient reduction at very high wind speeds. *J. Geophys. Res.*, **111**, C03024, doi:10.1029/2005JC003114.

Donelan, M.A., 1999: Wind-induced growth and attenuation of laboratory waves. *Wind-Over-Wave Couplings*, 183-194, Ed. S.G. Sajjadi, N.H. Thomas and J.C.R. Hunt, Clarendon Press, Oxford.

Donelan, M.A., Haus, B.K., Reul, N., Plant, W.J., Stiassnie, M., Graber, H.C., Brown, O.B., and E.S. Saltzman, 2004: On the limiting aerodynamic roughness of the ocean in very strong winds. *Geophys. Res. Letters*, 31, L18306, i:10.1029/2004GL019460.

Donnelly, W.J., Carswell, J.R., McIntosh, R.E., Chang, P.S., Wilkerson, J., Marks, F., and P.G. Black, 1999: Revised ocean backscatter models at C and Ku band under high-wind conditions. *J. Geophys. Res.*, **104**, 11485-11497.

Dulov, V.A., Kudryavtsev, V.N., and A.N. Bol·shakov, 2002: A field study of white caps coverage and its modulations by energy containing waves. in *Gas Transfer at the Water Surface*, edited by M. A. Donelan et al., AGU, Washington, D. C., pp. 187–192.

Emanuel, K.A., 1995: Sensitivity of tropical cyclones to surface exchange coefficients and a revised steady-state model incorporating eye dynamics. *J. Atmos. Sci.*, **52**, 3969-3976.

Frank, W.M., 1984: A composite analysis of the core of a mature hurricane. *Mon. Wea. Rev.*, **112**, 2401-2420.

Gemmrich, J., Banner, M., and C. Garrett, 2007: Spectrally resolved energy dissipation rate and momentum flux of breaking waves. *J. Phys. Oceanogr., 38,* Doi: 10.1175/2007JPO3762.1

Jarosz, E., Mitchell, D.A., Wang, D.W., and W.J. Teague, 2007: Bottom-up determination of air-sea momentum exchange under a major tropical cyclone. *Science*, **315**, 1707-1709.

Kaplan, J., and W.M. Frank, 1993: The large scale inflow-layer structure of Hurricane Frederic (1979). *Mon. Weath. Rev.*, **121**, 3-20.

Kolmogorov, A.N., 1949: Fragmentation of droplets in a turbulent flow. *Doklady Akademii Nauk SSSR*, **66**, 825-828.

Kolmogorov, A.N., 1954: On a new variant of the gravitational theory of motion of suspended sediments. *Izv. Akad. Nauk*

SSSR, Phys. Ser., **6**, 56-58.

Kudryavtsev, V.N., 2006: On effect of sea droplets on atmospheric boundary layer. *J. Geophys. Res.*, **111**, C07020, doi:10.1029/2005JC002970.

Kudryavtsev, V.N., and V.K. Makin, 2001: The impact of air-flow separation on the drag of the sea surface. *Boundary-Layer Meteorol.*, **98**, 155-171.

Kudryavtsev, V.N., and V.K. Makin, 2002: Coupled dynamics of short wind waves and air flow over long surface waves. *J. Geophys. Res.*, **107**, C12, 3209, doi: 10.1029/2001JC001251.

Kudryavtsev, V.N., and V.K. Makin, 2004: Impact of swell on marine atmospheric boundary layer. *J. Phys. Oceanogr.*, **34**, 934-949.

Kudryavtsev, V.N. and V.K. Makin, 2007: Aerodynamic roughness of the sea surface at high winds. *Boundary-Layer Meteorol.*, **125**, 289-303.

Kudryavtsev, V.N. and V.K. Makin, 2009: Model of the spume sea spray generation. *Geophys. Res. Lett.*, **36**, L06801, doi: 10.1029/2008GL036871.

Kukulka, T., Hara, T., and S.E. Belcher, 2007: A model of the air-sea momentum flux and breaking-wave distribution for strongly forced wind waves. *J. Phys. Oceanogr.*, **37**, 1811-1828.

Lighthill, J., 1999:, Ocean spray and the thermodynamic of tropical cyclones. *J. Eng. Math*, **35**, 11-42.

Makin, V.K., 2005: A note on drag of the sea surface at hurricane winds. *Boundary-Layer Meteorol.*, **115**, 169-176.

Makin, V.K., and V.N. Kudryavtsev, 2002: Impact of dominant waves on sea drag. *Boundary-Layer Meteorol.* **103**, 83-99.

Makin, V.K., and V.N. Kudryavtsev, 2003: Wind - over - waves coupling. In *Wind Over Waves II: Forecasting and Fundamentals of Application*, pp. 46-56, editors: S.G. Sajjadi and J.C.R. Hunt, Horwood Publishing Limited, Chichester, England.

Melville, W.K., and P. Matusov, 2002. Distribution of breaking waves at the ocean surface. *Nature*, **417**, 58-62.

Monin, A.S., and A.M. Yaglom, 1971: *Statistical Fluid Mechanics*. Cambridge: MIT Press, 769 pp.

Phillips, O.M., 1985: Spectral and statistical properties of the equilibrium range in wind generated gravity waves. *J. Fluid Mech.*, **156**, 505-531.

Powell, M.D., Vickery, P.J., and T.A. Reinhold, 2003: Reduced drag coefficient for high wind speeds in tropical cyclones. *Nature*, **422**, 279-283.

Powell, M.D., 2006: Drag coefficient distribution and wind speed dependence in tropical cyclones. *Final Report to the National Oceanic and Atmospheric dministration, Joint Hurricane Testbed Program*, Miami, 26.

Prandtl, L., 1949: *Fuhrer durch die Stromungslehre.* 3rd ed., F. Vieweg, Braunschweig.

Smith, M.H., Park, P.M., and I.E. Consterdine, 1993: Marine aerosol concentrations and estimated fluxes over the sea. *Quart. J. Roy. Meteorol. Soc.*, **119**, 809-824.

Taylor, P.A., Li, P.Y., and J.D. Wilson, 2002: Lagrangian simulation of suspended particles in the neutrally stratified surface layer. *J. Geophys. Res.*, **107**, D24, 4762, doi:10.1029/2001JD002049.

Wu, J., Murray, J.J. and R.J. Lai, 1984: Production and distributions of sea spray. *J. Geophys. Res.*, **89**, 8163-8169.

Appendix A
Governing Mass and Momentum Conservation Equations

The classical equations describing the dynamics of the turbulent flow with suspended heavy particles are introduced here following Monin and Yaglom (1971). These equations are then used for the construction of a "semi-empirical" model describing the mass and momentum conservation between wave crests and troughs.

The velocity of the mixture is defined as the weighted average over the mass value of the air and droplets velocities

$$v_j = \frac{\rho_a(1-s)}{\rho}u_j^a + \frac{\rho_w s}{\rho}u_j^w = u_j^a - \frac{\rho_w s}{\rho}a\delta_{j3}, \qquad (A.1)$$

where the second equality follows from (1.1) and (2.1). In the turbulent flow each of the quantities f is represented as a sum of its mean value $\overline{f}$ and its random fluctuation f' : $f = \overline{f} + f'$. Throughout the study we shall use the commonly accepted rules for the averaging of the governing equations for the turbulent flow.

A.1 Mass balance

Basic equations

The equations of the mass balance for the air flow and droplets read

$$\frac{\partial}{\partial t}[\rho_a(1-s)] + \frac{\partial}{\partial x_j}[\rho_a(1-s)u_j^a] = 0, \qquad (A.2)$$

$$\frac{\partial}{\partial t}(\rho_w s) + \frac{\partial}{\partial x_j}[\rho_w s(u_j^a - a\delta_{j3})] = 0. \qquad (A.3)$$

Here $x_{1,2}$ are the horizontal coordinates, x_3 is the vertical coordinate replaced in the main text by z. Adding these equations results in the equation of the mass balance for the mixture

$$\frac{\partial \rho}{\partial t} + \frac{\partial \rho v_j}{\partial x_j} = 0, \qquad (A.4)$$

and dividing these equations consequently by ρ_a and ρ_w and adding them gives the continuity equation for the mixture

$$\frac{\partial}{\partial x_j}[u_j^a - sa\delta_{j3}] = 0. \qquad (A.5)$$

Under stationary and spatially homogenous conditions averaged equations (A.4) and (A.5) with use of

$$\rho' = \triangle\rho s', \qquad (A.6)$$

$$\overline{\rho} = \triangle\rho\overline{s} + \rho_a, \qquad (A.7)$$

where $\triangle\rho = \rho_w - \rho_a$, read

$$\frac{\partial \overline{\rho v_3}}{\partial x_3} \equiv \frac{\partial}{\partial x_3}[\overline{\rho}\cdot\overline{u_3} - \rho_w\overline{s}a + \triangle\rho\overline{s'u_3'}] = 0, \qquad (A.8)$$

$$\frac{\partial}{\partial x_3}[\overline{u_3} - \overline{s}a] = 0. \qquad (A.9)$$

In (A.8) and (A.9) $\overline{s'u_3'}$ is the turbulent flux of the droplets concentration, and hereinafter we drop a superscript "a" from $u_3^a = u_3$. Far above the ocean surface the droplets concentration, its flux and the air vertical velocity turn to zero, therefore (A.8) and (A.9) are reduced to

$$\overline{\rho v_3} \equiv \overline{\rho}\cdot\overline{u_3} - \rho_w\overline{s}a + \triangle\rho\overline{s'u_3'} = 0 \qquad (A.10)$$

$$\overline{u_3} - \overline{s}a = 0. \qquad (A.11)$$

Equation (A.10) states that the vertical flux of mass of the mixture is zero, and equation (A.11) shows that the vertical velocity of the air should compensate the terminal fall velocity of droplets. Adding these equations the mass conservation equation for droplets is obtained

$$\overline{s'u_3'} - \overline{s}a(1-\overline{s}) = 0. \qquad (A.12)$$

The equation is valid above the wave crests, i.e., above the layer where the production of droplets takes place. In the ocean spume droplets are the main source of ocean spray at high wind speeds (Andreas, 1998; 2002). They are generated by the wind tearing off breaking wave crests. Being torn away from the breaking crest spume droplets are embedded into the airflow at the height of the breaking wave. K06 suggested to treat the process of the spume droplets generation as the volume source of droplets elevated above the surface.

Volume production of droplets

Let us consider the mass balance in the domain $\zeta(t, x_\alpha) < x_3 < h_b$, where $x_3 = \zeta(t, x_\alpha)$ is the sea surface displacement by the narrow band wind waves with the wavenumber in the range from $\mathbf{k}$ to $\mathbf{k} + d\mathbf{k}$, and h_b is the height of the breaking crest. The surface horizontal $u_{1,2}$ and vertical u_3 velocities could be written in the form

$$u_\alpha = u_\alpha^\zeta + u_\alpha',$$

$$u_3 = u_3^\zeta + u_3' + \overline{u}_3,$$

where the superscript ζ indicates the wave orbital surface velocity obeying the surface kinematic boundary condition $u_3^\zeta = \partial\zeta/\partial t + u_\alpha^\zeta\partial\zeta/\partial x_\alpha$, $\overline{u}_3$ is the mean vertical air velocity associated with the terminal fall velocity of droplets, and u' is the random velocity associated with the surface disruption (tearing) due to the generation of droplets.

The integral mass balance equation below breaking wave crests can be found by the integration of equation (A.4) from the surface ζ_{t,x_α} to the level $x_3 = h_b$ just above wave breaking crests. Performing the ensemble averaging and assuming stationary and spatially homogenous conditions we obtain

$$-(\overline{\rho' u_n'})_\zeta - (\overline{\rho}\cdot\overline{u_3})_\zeta + \rho_w a\overline{s}_\zeta + \overline{\rho v_3}|_{x_3=h_b} = 0, \qquad (A.13)$$

where u_n is the air velocity component normal to the surface, and $\overline{s}_\zeta$ is the mean concentration of droplets at the surface. The first term in (A.13) describes the injection of droplets into the airflow from the sea surface, which occurs predominantly from breaking wave crests at $x_3 = h_b$. Performing the same

operations with the continuity equation (A.5) we obtain $\overline{u}_{3\zeta} = a\overline{s}_\zeta$ at the surface. Substituting this relation into (A.13) and taken into account (A.6)-(A.7) the mass conservation equation reads

$$-\Delta\rho(\overline{s'u'_n})_\zeta + \Delta\rho a\overline{s}_\zeta(1 - \overline{s}_\zeta) + \overline{\rho v_3}|_{x_3=h_b} = 0. \qquad (A.14)$$

Since the mass flux above the wave crests is vanished $\overline{\rho v_3}|_{x_3=h_b} = 0$, see equation (A.10), equation (A.14) describes the obvious fact that all droplets injected from the surface inevitably fall back to the water

$$(\overline{s'u'_n})_\zeta - a\overline{s}_\zeta(1 - \overline{s}_\zeta) = 0. \qquad (A.15)$$

We consider the mean airflow in the Cartesian coordinate system above the mean water surface $x_3 = 0$. As stated above droplets are injected from breaking crests well above the mean water surface. Therefore, the droplets flux can by no means be treated as a flux through the water surface $x_3 = 0$; it is spread over the height $0 < x_3 < h_b$. The dynamics of the turbulent flow with suspended particles between breaking wave crests and troughs is complicated and we are not aware of any model approach describing such problem. Therefore, we shall study this problem on a semi-empirical level. We assume that both the turbulent flux $\overline{s'u'_3}$ and the concentration $\overline{s}$ of droplets varies continually in the layer $0 < x_3 < h_b$ from their values at $x_3 = h_b$ to that at $x_3 = 0$. The turbulent flux of droplets at $x_3 = 0$ must be vanished as it was suggested that droplets are produced at $x_3 = h_b$. Simulating production of droplets as a jet located at $x_3 = h_b$, we introduce a differential equation describing the distribution of droplets in the layer $0 < x_3 < h_b$ in the following form

$$\frac{\partial}{\partial x_3}(\overline{s'u'_3} - a\overline{s}) = F_s\delta(x_3 - h_b) \qquad (A.16)$$

with the surface boundary condition $\overline{s'u'_3} = 0$ at $x_3 = 0$. Here $F_s = (\overline{s'u'_n})_\zeta$ is the volume flux of spume droplets from breaking wave crests, $\delta(x)$ is the Dirac delta function, and terms containing s^2 are neglected because $s \ll 1$. Equation (A.16) being integrated from $x_3 = 0$ to infinity reduces to (A.15), and from $x_3 = h_b$ to infinity - to (A.12). We consider equation (A.16) as the mass conservation equation valid in the whole domain below and above wave crests.

A.2 Momentum balance

The horizontal momentum conservation equation for the fluid with suspended particles in terms of the mixture density ρ and the mixture velocity v_j defined by (1.1) and (A.1) is similar to the corresponding equation for the pure fluid (Monin and Yaglom 1971)

$$\frac{\partial}{\partial t}(\rho v_\alpha) + \frac{\partial}{\partial x_j}[\rho v_\alpha v_j + p\delta_{\alpha j} - \sigma_{\alpha j}] = 0, \qquad (A.17)$$

where p is the total pressure and σ_{ij} is the tensor of the viscous stress.

Above wave crests

Performing the ensemble average of (A.17) and assuming stationary and spatially homogenous conditions we obtain the following equation valid above the wave crests

$$\frac{\partial}{\partial x_3}[\overline{\rho}\overline{u'_1u'_3} + (\overline{\rho}\cdot\overline{u}_1\cdot\overline{u}_3 + \overline{u}_1\overline{\rho'u'_3} - \rho_w a\overline{s}\cdot\overline{u}_1)] = 0, \qquad (A.18)$$

where terms containing second and third moments of the density fluctuation and the horizontal velocity fluctuation, i.e., $\overline{\rho'u'_1u'_3}$, $\overline{\rho'u'_1u'_3}$ and $\rho_w a\overline{s'u'_1}$, as well as the viscous stress are neglected. Due to equations (A.6), (A.7) and (A.10) the terms enclosed in parenthesis in (A.18) are canceled and it is reduced to

$$\frac{\partial}{\partial x_3}(\overline{\rho}\overline{u'_1u'_3}) = 0, \qquad (A.19)$$

i.e. the turbulent stress is constant over height: $\overline{\rho}\overline{u'_1u'_3} = const$.

Between wave crests and troughs

The integral momentum balance equation of the mixture below the breaking crests can be found by the integration of equation (A.17) from the sea surface $x_3 = \zeta$ to the level $x_3 = h_b$. After the ensemble average and assuming stationary and spatially homogenous conditions we obtain

$$-\overline{\rho(u^0_\alpha + u'_\alpha)(u'_n + \overline{u_3} - \rho_w/\rho\cdot as)}|_{z=\zeta} + \overline{p\partial\zeta/\partial x_\alpha}|_{z=\zeta} + \overline{\rho u_\alpha v_3}|_{z=h_b} = 0. \qquad (A.20)$$

Taking into account that $\overline{\rho(u'_n + \overline{u_3} - \rho_w/\rho\cdot as)}|_{z=\zeta} = 0$ (since the mass flux through the surface is zero, see equation (A.10)) and neglecting the third order moments and the horizontal flux of droplets at the surface, equation (A.20) is reduced to

$$-\overline{\rho}\overline{u'_\alpha u'_n}|_{x_3=\zeta} + \overline{p\partial\zeta/\partial x_\alpha}|_{x_3=\zeta} + \overline{\rho}\overline{u'_\alpha u'_3}|_{x_3=h_b} = 0. \qquad (A.21)$$

This equation shows that the momentum flux at the surface is supported by the tangential stress and the form drag, and that the effect of droplets appears explicitly through the mixture density $\overline{\rho}$.

The form drag is supported by the momentum flux to a regular or streamlined wavy surface by the non-separated sheltering mechanism (Belcher and Hunt 1993) and by the separation of the air flow from breaking waves (KM01, Makin and Kudryavtsev 2002). Short waves provide the main contribution to the form drag, as shown by Makin and Kudryavtsev (2003). These short waves are distributed uniformly along the sea surface and the stress they support could be treated as the force acting on the mean surface. For high wind speeds a significant part of the stress is supported by the separation of the air flow (e.g., Figure 5 from KM07). The separation of the airflow results in the action of the pressure drop Δp_s on the forward side of a breaking wave. As shown by KM01, this component of the form drag supported by wind waves in the wavenumber range from

k to **k** + *d***k** reads

$$\overline{p\partial\zeta/\partial x_\alpha}|_{z=\zeta} = \Delta p_s h_b L_b, \qquad \text{(A.22)}$$

where L_b is the length of wave breaking crests per unit surface area. Following the same approach as was used for the derivation of the droplets conservation equation (A.16), we consider the airflow separation stress as a stress uniformly distributed in the layer $0 < x_3 < h_b$. Then the momentum conservation equation, which is valid above and below breaking crests, takes the form

$$\frac{\partial}{\partial x_3}(\overline{\rho u_1' u_3'}) = -\Delta p_s h_b L_b \delta(x_3 - h_b). \qquad \text{(A.23)}$$

At $x_3 > h_b$ this equation is reduced to (A.19), and being integrated from some level above h_b to the surface it reduces to (A.21).